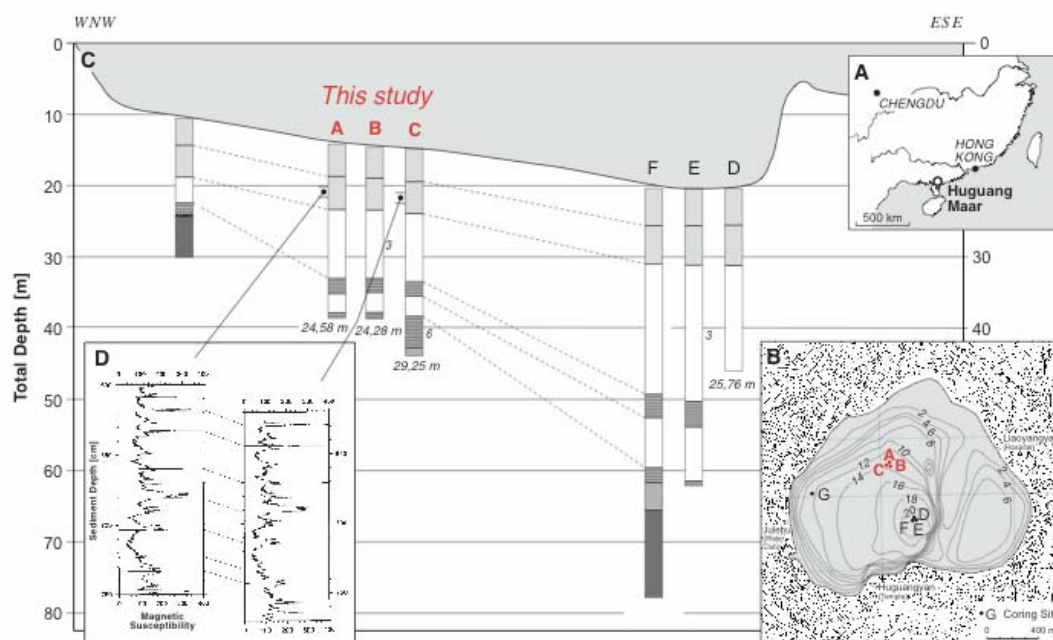


### Regional Setting and Climatology

Lake Huguang Maar, a volcanic crater lake, is situated on the Leizhou Peninsula (Supp. Fig. 1 and 2), which is a part of the Leiqiong Volcanic Field (LQVF)<sup>1</sup>. The LQVF comprises the central part of the Beibuwan Basin, which has developed as an extensional basin on a passive continental margin<sup>2</sup>. Volcanic activity in this area occurred from 28 to 0.1 Ma, with most exposed basalts dating from the Early to Middle Pleistocene (1.8–0.4 Ma)<sup>3</sup>. The mafic volcanic rocks of LQVF are dominated by olivine tholeiites, with ilmenite and titanomagnetite as the main Fe-oxides<sup>3</sup>. Ilmenite is paramagnetic at room temperature and is therefore not of great importance for the rock magnetic signal of the sediment sequence in Lake Huguang Maar.

Among the identified volcanic structures in the LQVF, Huguang Maar (Supp. Fig. 1) is the deepest recent crater lake<sup>1</sup>, with a diameter of ~ 1.7 km and a depth of ~ 20 m. K/Ar dated basalts from the volcanoclastic breccia of the crater rim have yielded an age of about 127 ka, suggesting lake formation at roughly that time<sup>4</sup>.

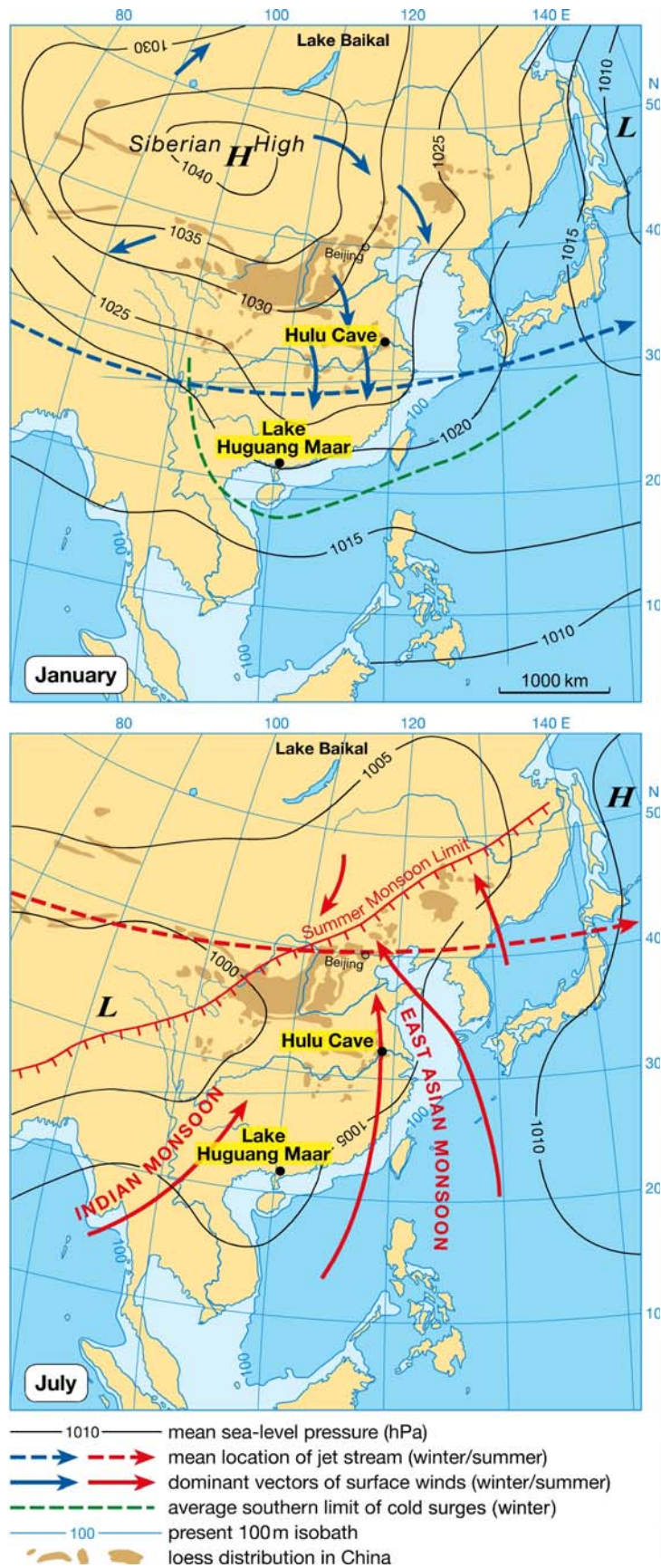


**Supp. Fig. 1:** (A) Schematic map of Southeast China and location of Lake Huguang Maar. (B) Cross section bathymetry of Lake Huguang Maar and the positions of the coring sites in the lake. The sediment cores from site HUG-ABC (water depth of 13.3 m) used in this study are highlighted in red. (C) Water depth profile, simplified stratigraphy and correlation between the individual sediment cores from Lake Huguang Maar. (D) Comparison between the magnetic susceptibility logs of two of the parallel cores from site HUG-ABC.

The site is directly influenced by the East Asian monsoon and, to a lesser extent, by the Indian monsoon (Supp. Fig. 2). Today, strong winter winds from the north and northeast prevail from November until March, while the site receives much of its precipitation from the summer position of the monsoon rainbelt in South China<sup>5</sup>. The local topography is such that the lake surface is most exposed to winds from the North. Combined with the fact that continuous strong northerly

winds are associated with the winter (rather than summer) monsoon, this makes the lake vulnerable to wind-driven mixing during the winter. In years of strong winds associated with the winter monsoon, the lake is fully overturned, and the bottom waters are charged with oxygen, which leads to higher respiration rates, a lower sedimentary concentration of organic carbon, and other indicators of oxic sedimentary conditions. In the case of a weaker winter monsoon and reduced wind stress, the absence of mixing causes the bottom water to become anoxic, leading to higher sedimentary total organic carbon (TOC) and other indicators of anoxic sedimentary conditions.

The monsoon winds are necessarily a response to pressure gradients, requiring that we also consider the Siberian high pressure system, which is the counterpart to the low-pressure ITCZ in driving the wintertime monsoon winds. As confirmed with numerical models<sup>6</sup>, northern hemisphere cooling would be expected to strengthen the Siberian High as the ITCZ shifts southward. We do not yet understand why the ITCZ has migrated as it has over the Holocene, as the Greenland ice cores indicate no major Holocene cooling in the northern hemisphere. Nevertheless, we would predict that our interpreted migrations in ITCZ location are coupled to parallel changes in the Siberian High. If the Siberian high were to remain static as the ITCZ migrated southward, the wintertime pressure gradient would have dropped, potentially weakening winter winds over the Holocene, in opposition to the evidence from Huguang Maar.

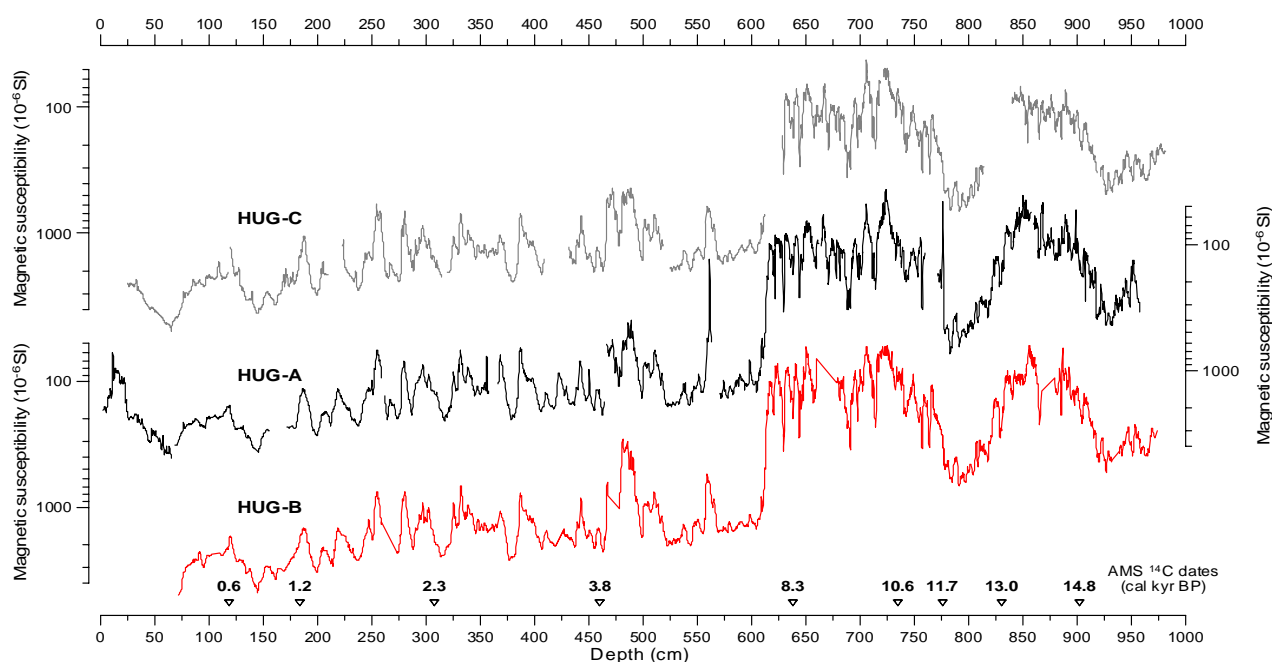


**Supp. Fig. 2:** Mean meteorological features over Southeast Asia (after<sup>7-9</sup>). The locations of Lake Huguang Maar, Hulu Cave and the loess plateau are shown.

### Core description

In 1997, a team from GeoForschungsZentrum Potsdam and the Chinese Academy of Sciences drilled seven sediment cores (HUG-A to -G) from three different sites in the lake. A high-precision USINGER piston corer was used to recover sediment profiles with a maximum length of 57.8 m<sup>1</sup>.

Cores HUG-A to -C used for this study were recovered from a water depth of 13.4 m (Supp. Fig. 1, 3). To facilitate the comparison among the individual cores, the HUG-A and -B were shifted to directly match the common depth scale of HUG-C. The transfer functions are based on correlation of magnetic susceptibility features, which are highly reproducible among the individual cores (Supp. Fig. 3). The magnetic properties S-ratio and magnetic susceptibility are based on a composite record from HUG-A and HUG-C, and  $\mu$ XRF-based Ti content was analyzed on core HUG-B.



**Supp. Fig. 3:** Comparison among the magnetic susceptibility logs of the parallel cores from site HUG-A, -B, and -C. To facilitate the comparison among the individual cores, the depths of HUG-A and -B were recalculated to directly match the depth scale of HUG-C. Magnetic susceptibility features in all three cores are highly reproducible. AMS <sup>14</sup>C dated levels with their respective ages are indicated.

### Sediment composition

The cored sediment from Lake Huguang Maar is composed of homogeneous greenish-black algal 'gyttja' (organic-rich mud) with some dispersed authigenic siderite. The  $\delta^{13}\text{C}$  of the organic matter ranges from -18 to -22 ‰, and C/N ratios are generally below 15, both of which indicate that most of the organic fraction is produced by algae within the lake and is not derived from local terrestrial plants. As the inner slope of the lake crater is densely vegetated (evergreen sub-tropical forest) and as there are no coherent stream inputs, it is rather unlikely that local runoff from within the catchment contributes significantly to the sediment deposition. Furthermore, the temporal variability of the terrigenous input to Lake Huguang Maar is not effectively explained by local erosional changes, since no dramatic changes in the vegetation occurred between the Holocene and the Glacial at this site; the ratio of wooden to non-wooden taxa increases only modestly from the last glacial (0.45) to the Holocene (0.65), with no significant change within the Holocene<sup>1</sup>.

Moreover, the pollen signal is regional, and the local catchment of the lake should be even more densely vegetated due to its sheltered position and higher local moisture availability.

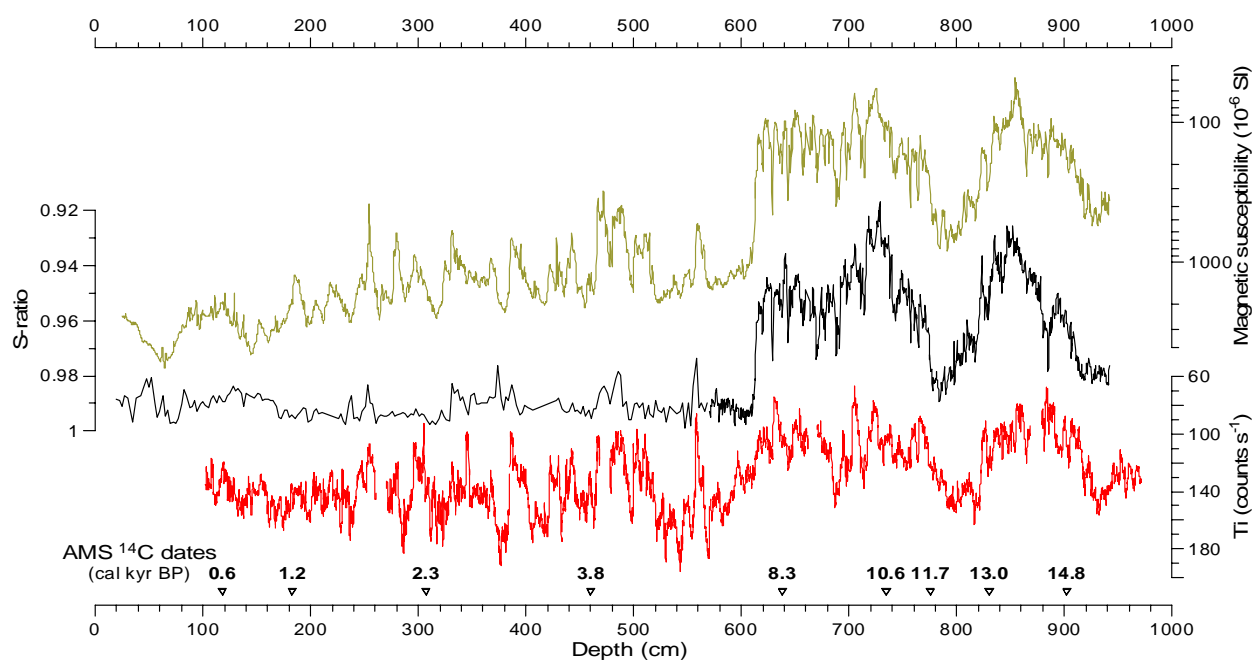
The anthropogenic influence seen in pollen records from the lake (an increase in anthropogenic species) reflects regional trends as well. The pollen data indicate that the anthropogenic influence increases after 2.5 kyr<sup>1</sup>. This may contribute to the gradual increase in sediment input to the lake over the last 2.5 kyr of the Huguang Maar records, largely through regional effects on eolian transport, but it cannot explain the decadal to centennial variability in the rock magnetic parameters and the Ti record over this period.

Today, dust flux in coastal South China is 4.6 mg cm<sup>-2</sup> yr<sup>-1</sup> on average (varying between 1.1 and 12 mg cm<sup>-2</sup> yr<sup>-1</sup>)<sup>10, 11</sup>. This is comparable to the siliciclastic flux to Lake Huguang Maar, which varies between 5 and 10 mg cm<sup>-2</sup> yr<sup>-1</sup> during the Holocene and between 10 and 20 mg cm<sup>-2</sup> yr<sup>-1</sup> during glacial times. The glacial/Holocene difference in Huguang Maar is consistent with other lake and marine records from East Asia<sup>12-17</sup>. Thus, all evidence suggests that the Huguang Maar terrigenous sediment accumulation is dominated by eolian inputs.

Due to the large seasonal temperature gradient in the region (ranging from 16°C in January to 29°C in July), the water column of Lake Huguang Maar is characterized by changing stratification through the year. The least stable water column occurs during the winter and early spring. In contrast, the lake is more stratified (with a stronger thermocline) in the summer, making it less sensitive to typhoons. Today, despite the occurrence of typhoons in this region, summertime suboxia is the norm in the lake and is recorded as such in the surface sediments. Due to the very close position of the site to the South China Sea coast, the summer monsoon is not expected to transport significant dust loads. Thus, the lake sediment redox conditions and Ti content are most sensitive to the winter monsoon activity, with little influence from the summer monsoon or other summertime phenomena.

Subsequent to the increase in oxygenation of the lake in the mid-Holocene, the S-ratio is nearly saturated (i.e. at its upper limit of 1). Nevertheless, supplementary rock magnetic data show that, in the younger Holocene sediments (0 – 600 cm, Supp. Fig. 3), some of the largest S-ratio variations parallel variations in magnetic susceptibility and Ti. Magnetic susceptibility is affected by both oxygenation and aeolian inputs, while Ti is affected solely by aeolian inputs. Thus, this suite of measurements suggests that the correspondence between better oxygenation of the lake bottom and enhanced dust transport that is found for the Glacial and Younger Dryas holds true for the Mid- and Late Holocene as well (Supp. Fig. 4).



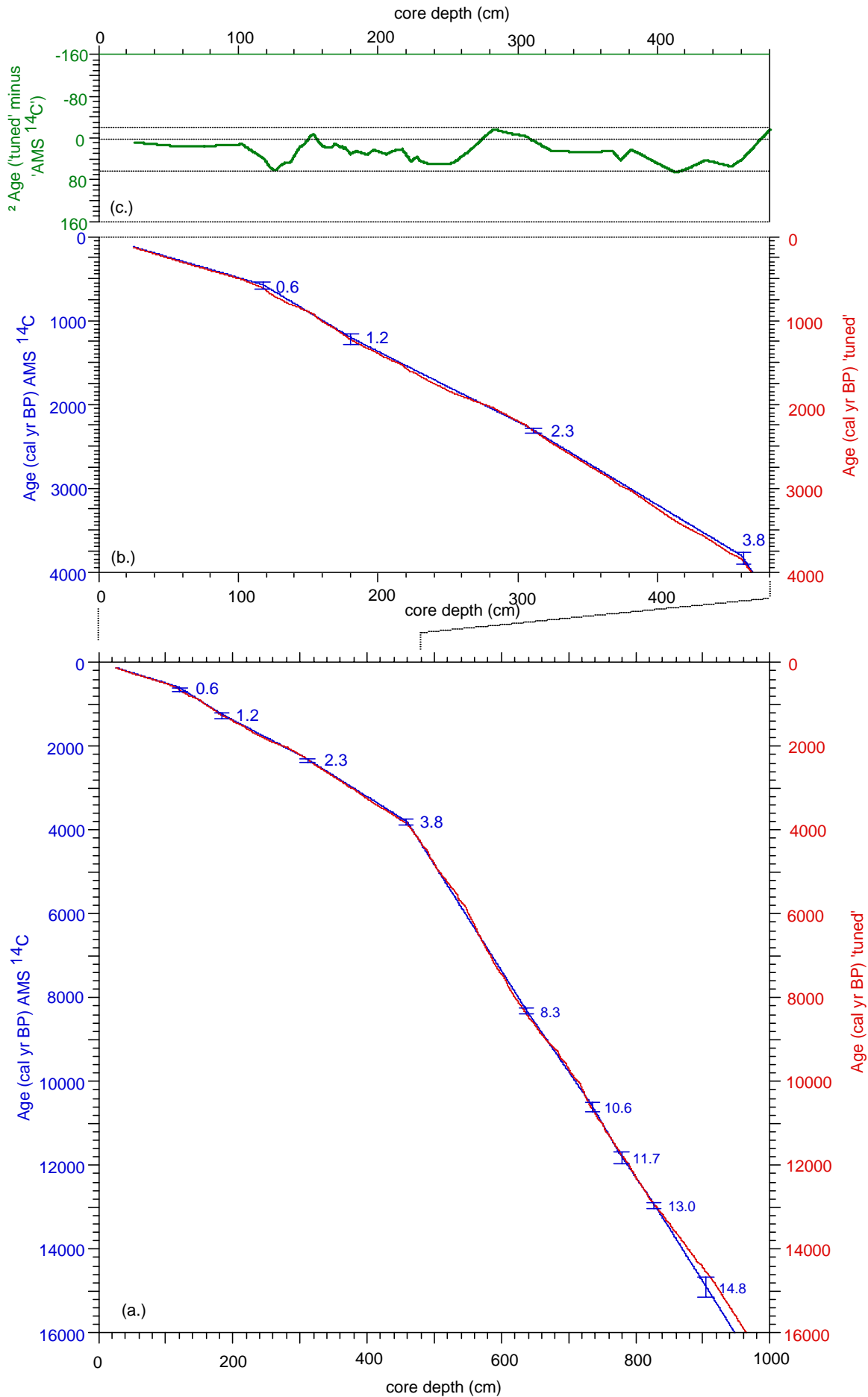


**Supp. Fig. 4:** Stratigraphic distribution of rock magnetic parameters, magnetic susceptibility and S-ratio, and Ti content from the Lake Huguang Maar sediment sequence HUG-ABC. AMS <sup>14</sup>C dated levels with their respective ages are indicated.

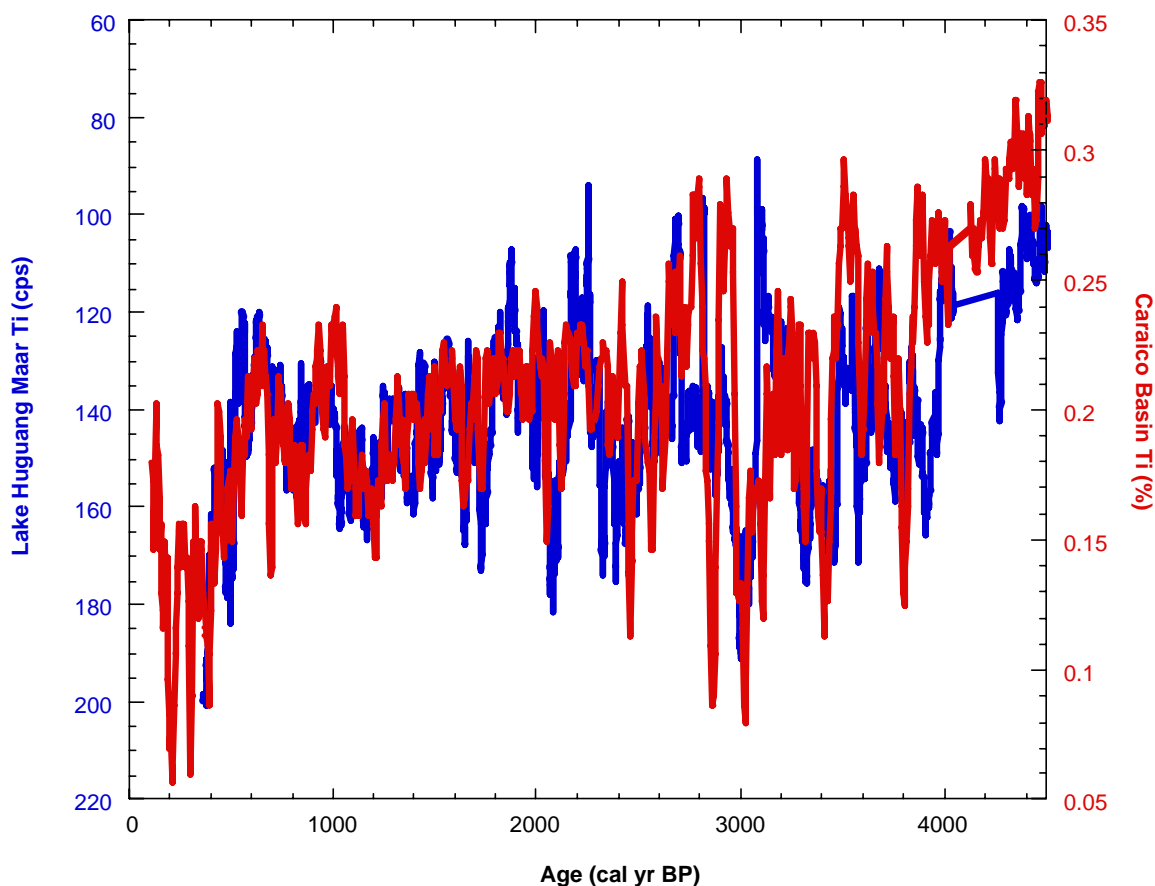
### Age Model

The sediment section of Lake Huguang Maar which extends back to 16.2 kyr (Supp. Fig. 5) is characterized by sedimentation rates ranging from 41 cm kyr<sup>-1</sup> prior to the Bølling-Allerød to 112 cm kyr<sup>-1</sup> during the past 4000 years. The initial age model is based on 5 AMS <sup>14</sup>C dates of leaves and 4 of bulk sediment, with dating errors of less than ±160 years within the 1 sigma interval of the AMS <sup>14</sup>C method (Supp. Figure 5a). Given the evident correlation between the Huguang Maar records and the Hulu Cave oxygen isotope record<sup>18</sup> during Termination I and the Bølling-Allerød, the age model of the Huguang Maar record was subsequently adjusted by visually matching common inflection points and interpolating between these points (Supp. Fig. 5a-c). In the Younger Dryas and Holocene, we used the well-dated Ti record from Cariaco Basin, off Venezuela<sup>19</sup> for minor age adjustments (Supp. Fig. 6). The resulting stratigraphy deviates during the past 4000 years by no more than 70 yr from the original <sup>14</sup>C based age model and is thus fully consistent with that model within its window of uncertainty (Supp. Fig. 5c), with one exception at 14.9 kyr (Supp. Fig. 5c).

The comparison between the Cariaco and the Huguang Maar records in the critical time interval of the AD 800's in a Cariaco age versus Huguang Maar depth plot, anchored by the key AMS <sup>14</sup>C date of the century, is shown in Supp. Fig. 7. The relationship between the records is rather clear and by no means forced by an altered age model.

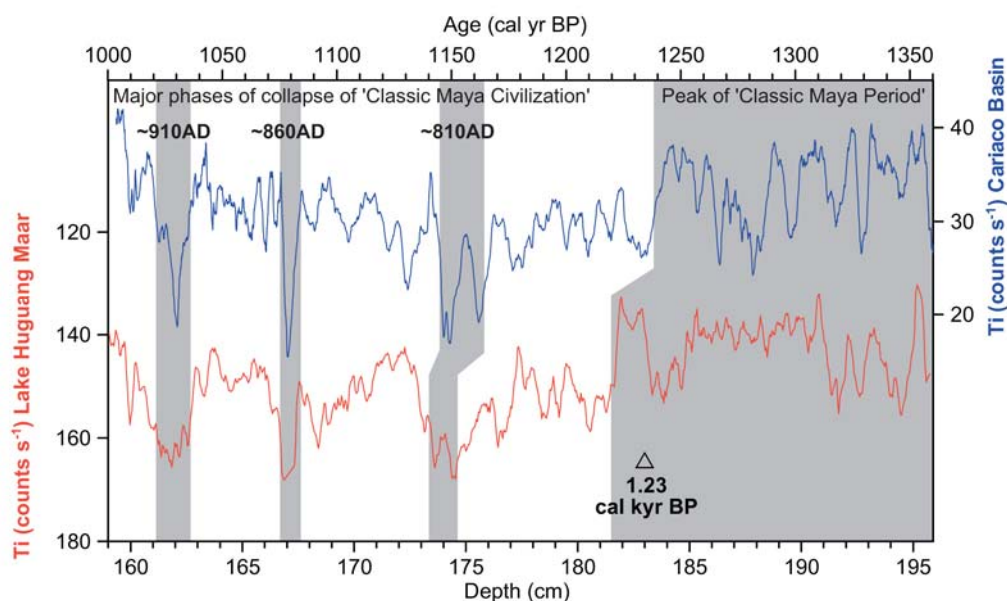


**Supp. Fig. 5:** Age model for the Lake Huguang Maar record. (a) Age depth plot for the entire record. Blue line: AMS  $^{14}\text{C}$  (in cal yr) versus depth. AMS  $^{14}\text{C}$  dates are given with 2 sigma error bar. The red line is the tuned age model based on the minor adjustment to the Cariaco and Hulu Cave records. The ‘tuning’ was conducted always within the error bar of the AMS  $^{14}\text{C}$  age model. (b) Same as (a) but blown up for the past 4000 years. The red line is the tuned age model based on the minor adjustment to the Cariaco Basin record. (c) Age offset of our age model from a linear interpolation between the dates during the past 4000 years. The maximum offset is 70 years, whereas ‘the average offset’ is less than 30-40 years.



**Supp. Fig. 6:** Lake Huguang Maar Ti record versus Cariaco Basin Ti record during the past 4500 years. For explanation see text.





**Supp. Fig. 7:** Lake Huguang Maar Ti record versus depth anchored with an AMS  $^{14}\text{C}$  date to the Cariaco basin Ti record versus age<sup>19</sup>.

### Holocene redox changes at Lake Huguang Maar

The S-ratio (and magnetic susceptibility) changes from 15.5 to 8 kyr suggest lake redox changes (consistent with the TOC changes) that would indicate stronger winter monsoon winds when the summer monsoon was weaker. After 8 kyr, our reliance on the TOC data may be considered weaker, as the TOC changes might be due to some process other than  $\text{O}_2$ -related preservation, such as changes in productivity or dilution. A number of points argue against this concern:

(1.) Magnetic properties show a strong affinity to different water depths (higher dissolution of magnetic particles at greater water depths), whilst other sediment properties (dry density, water content) do not – this makes a strong case for mixing, not productivity.

(2.) TOC/TN ratio, a rough indicator of the relative contributions of aquatic algae and higher terrestrial plant to the sediments, is remarkably constant (with a slight, steady increase due to long-term diagenetic effects) from the most recent samples far back into the last Glacial.

(3.) In sediment intervals coinciding with times of high S-ratio, low TOC, high Ti, and weak summer monsoons, siderite is present. Work in other lakes indicates that siderite is the common result of mixing of suboxic waters (which occur today during the summer in Huguang Maar) with overlying waters<sup>20</sup>, such that wintertime wind mixing would help to explain this observation. Although the amount of primarily precipitated siderite has been altered diagenetically, lower lake productivity fails to explain the occurrence of siderite during times of high Ti input and weak summer monsoons.

(4.) Reflectance measurements of terrestrial organic matter reveal a much larger fraction of wind-derived, oxidized biogenic particles during times with reduced summer monsoon activity that seems difficult to explain solely by vegetation and summer monsoon changes<sup>21</sup>.

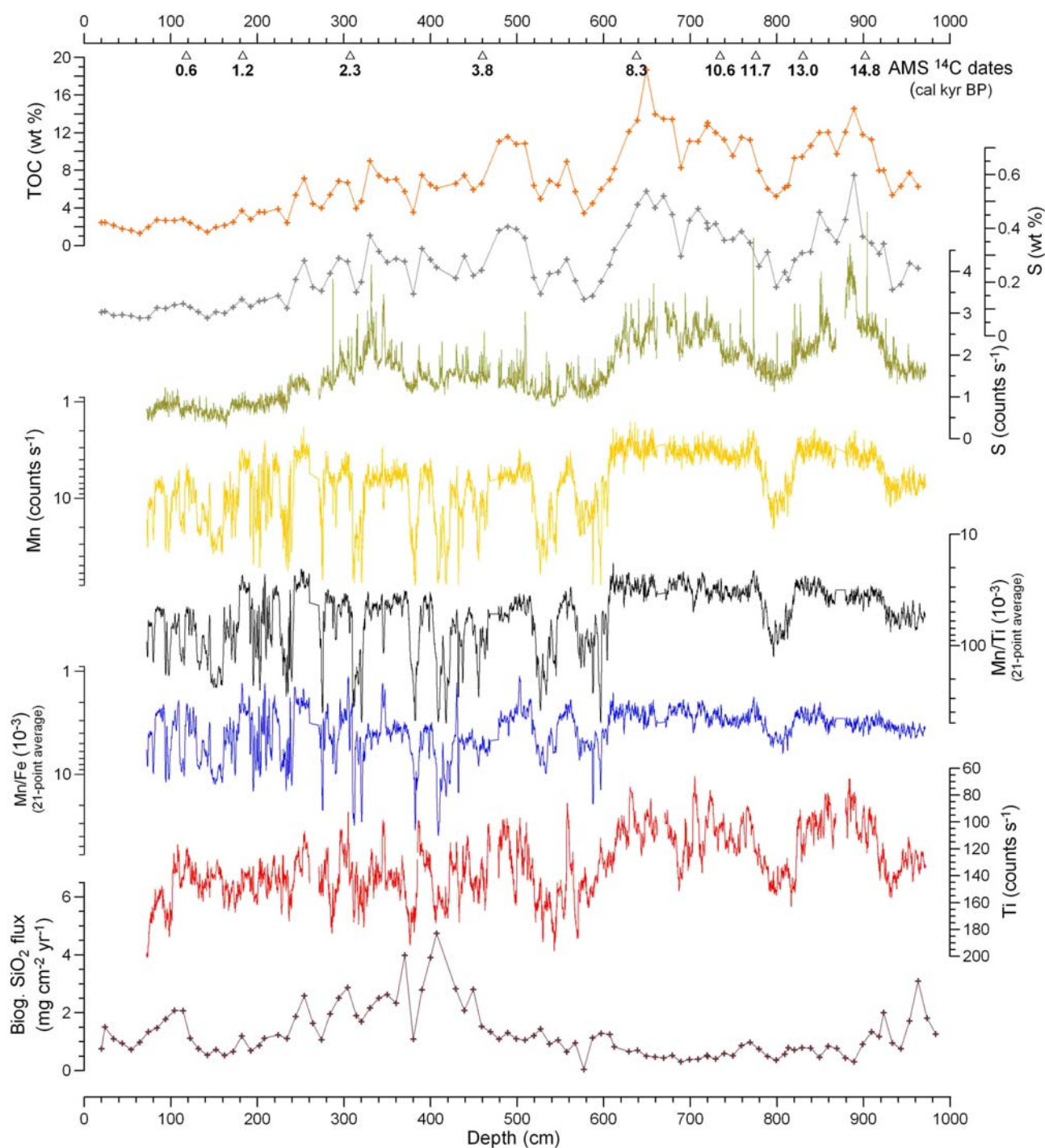
(5.) Dilution is not a plausible explanation for the TOC changes, which are several fold too large to be explained by accumulation rate changes. Note also that TOC content is typically of greater interest for reconstructing redox conditions than accumulation rate, as more rapid burial can

increase burial efficiency.

(6.) The manganese redox chemistry also argues for changes in lake redox conditions and supports the notion that these redox changes are the result of changes in lake mixing and not productivity. Sedimentary profiles of Mn and Fe have been used as indicators of changing redox conditions in lakes (e.g.<sup>22</sup>). These authors (and many others, e.g.<sup>20, 23</sup>) have shown that “Mn concentration peaks are recording oxidation events in the hypolimnion” in lakes comparable to Lake Huguang Maar. Schaller *et al.*<sup>22</sup>, working in a Swiss lake, find that “Oxygenation input by wind mixing produce a particle flux of MnO<sub>2</sub>, which could be partially preserved in the sediment as MnCO<sub>3</sub>.” They find further that, ” [sediment] Mn values are correlated to average deep water oxygen concentrations,” and that “the distribution of the data suggests two distinct groups: (1) constant low [sedimentary] Mn values at low oxygen concentrations indicating incomplete mixing and (2) high Mn concentrations at high average O<sub>2</sub> values indicating strong winter storms with complete mixing”.

In Supp. Fig. 8, we show the sedimentary profiles of Mn (counts/s) and the Mn/Ti and Mn/Fe ratios. We observe higher Mn concentrations and higher Mn/Ti and Mn/Fe ratios during the YD period, when the S-ratio is higher and TOC is lower. At 7.8 kyr, when the S-ratio loses its sensitivity as a result of somewhat higher lake oxygen levels, the Mn values go up, as expected. During the past 8000 years (and the entire record), the Mn concentrations increase when TOC (and S) concentrations decrease (and magnetic susceptibility and Ti content increase). This argues that the TOC is indeed responding to redox history, and it also argues (by analogy to the Swiss system), that lake mixing is responsible for the redox changes. The Mn maxima occur during times of Ti maximum, as to be expected. However, detailed comparison between the Mn and Ti concentration records and the elemental ratios Mn/Ti and Mn/Fe show that the Mn changes are not simply a function of input correlated with Ti. Note, in addition, that Mn collapses to baseline levels, suggestive of no mechanism for oxidation and resulting burial when the winter monsoon is weak (Supp. Fig. 8).

(7) Also plotted in Supp. Fig. 8 is the accumulation rate of biogenic silica. This is a particularly important indicator for our study. Biogenic opal flux provides an indication of productivity changes. While preservation can certainly vary for biogenic opal, there is no particular reason that it should vary with the climatic effects on Huguang Maar, such as mixing and redox state. Biogenic opal accumulation changes little over the period of interest (except for a maximum at ~3 kyr) and provides no indication that one might explain the apparent lake redox changes (or the TOC and sulfur records) as the result of large-scale climate-linked productivity changes. This is consistent with previous arguments we have made about productivity in the lake.

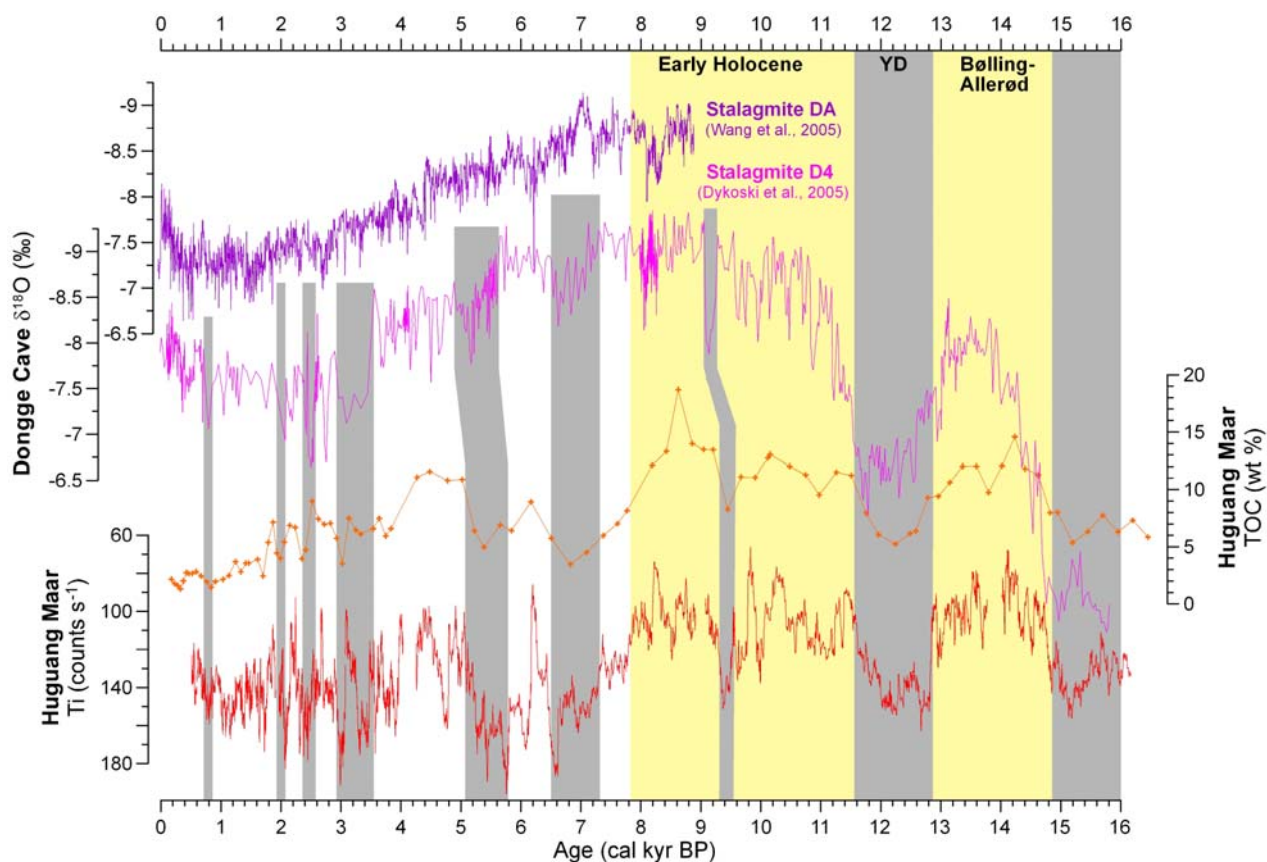


**Suppl. Fig. 8:** Lake Huguang Maar TOC (%), sulfur (% from IR-spectrometry and  $\mu$ XRF counts/s), Mn (counts/s), Mn/Ti, Mn/Fe, Ti (counts/s) and biogenic opal flux records versus depth. AMS  $^{14}\text{C}$  ages are at the top.

### Comparison to the Dongge Cave speleothem records

We compare in Suppl. Fig. 9 the Lake Huguang Maar Ti record to the Dongge Cave speleothem records (stalagmite D4<sup>24</sup> and DA<sup>25</sup>) for the Holocene interval. Below, we tentatively note several late Holocene intervals of potential correlation between stalagmite D4 from Dongge and the Huguang Maar Ti record, which would link periods of weak summer monsoon with a strong winter summer monsoon – the same sense of (anti)correlation that is much more clear in the earlier Holocene. Interestingly, the Ti record does not clearly show the late Holocene trend evident in both

Dongge records, while the magnetic susceptibility, TOC and sulfur records do, again in the expected sense of summer/winter monsoon anti-correlation.



**Suppl. Fig. 9:** Lake Huguang Maar titanium and TOC records versus the speleothem records D4<sup>24</sup> and DA<sup>25</sup> from Dongge Cave during the past 16 kyr. Shadings reflect phases of low precipitation as seen in the Dongge Cave data in relation to high titanium and low TOC (stronger winds, more wind stress and mixing of the lake, more oxygen supply to the deep lake and more TOC degradation).

## References

1. Mingram, J. et al. The Huguang maar lake - a high-resolution record of palaeoenvironmental and palaeoclimatic changes over the last 78,000 years from South China. *Quat. Int.* 122, 85-107 (2004).
2. Ma, X. & Wu, D. Cenozoic extensional tectonics in China. *Tectonophysics* 133, 243-255 (1987).
3. Ho, K.-S., Chen, J.-C. & Juang, W.-S. Geochronology and geochemistry of the late Cenozoic basalts from the Leiqiong area, southern China. *Journal of Asian Earth Science* 18, 307-324 (2000).
4. Fong, G. R. Cenozoic basalts in southern China and their relationship with tectonic environment. *Journal of Zhongshan University* 27, 93-103 (1992).
5. Ding, Y. *Monsoons over China* (Kluwer Academic Publishers, Dordrecht, Boston, London, 1994).
6. Zhang, R. & Delworth, T. L. Simulated tropical response to a substantial weakening of the Atlantic thermohaline circulation. *Journal of Climate* 18, 1853-1860 (2005).
7. Porter, S. C. & An, Z. Correlation between climate events in the North Atlantic and China during the last glaciation. *Nature* 375, 305-308 (1995).



8. Xiao, J. et al. Eolian quartz flux to Lake Biwa, Central Japan, over the past 145,000 years. *Quat. Res.* 48, 48-57 (1997).
9. Araguás-Araguás, L., Froehlich, K. & Rozanski, K. Stable isotope composition of precipitation over southeast Asia. *J. Geophys. Res.* 103, 28,721-28,742 (1998).
10. Gao, Y. & Anderson, J. R. Characteristics of Chinese aerosols determined by individual-particle analysis. *J. Geophys. Res.* 106, 18,037-18,045 (2001).
11. Cao, J. et al. Characterization of dust storms to Hong Kong in April 1998. *Water Air and Soil Pollution* 3, 213-229 (2003).
12. Hodell, D. A. et al. Paleoclimate of Southwestern China for the past 50,000 yr inferred from lake sediment records. *Quat. Res.* 52, 369-380 (1999).
13. Hovan, S. A., Rea, D. K. & Pisias, N. G. Late Pleistocene continental climate and oceanic variability recorded in Northwest Pacific sediments. *Paleoceanography* 6, 349-370 (1991).
14. Kohfeld, K. E. & Harrison, S. P. Glacial-interglacial changes in dust deposition on the Chinese Loess Plateau. *Quat. Sci. Rev.* 22, 1859-1878 (2003).
15. Mahowald, N. et al. Dust sources and deposition during the last glacial maximum and current climate: A comparison of model results with paleodata from ice cores and marine sediments. *J. Geophys. Res.* 104, 15,895-15,916 (1999).
16. Nilson, E. & Lehmkuhl, F. Interpreting temporal patterns in the late Quaternary dust flux from Asia to the North Pacific. *Quat. Int.* 76/77, 67-76 (2001).
17. Ding, Z., Rutter, N., Han, J. & Liu, T. A coupled environmental system formed at about 2.5 Ma in East Asia. *Palaeogeogr., Palaeoclimatol., Palaeoecol.* 94, 223-242 (1992).
18. Wang, Y. J. et al. A high-resolution absolute-dated Late Pleistocene monsoon record from Hulu Cave, China. *Science* 294, 2345-2348 (2001).
19. Haug, G. H. et al. Climate and the collapse of Maya civilization. *Science* 299, 1731-1735 (2003).
20. Stumm, W. & Morgan, J. J. *Aquatic Chemistry* (John Wiley & Sons, Inc., New York, 1996).
21. Fuhrmann, A. et al. Variations in organic matter composition in sediments from Lake Huguang Maar (Huguangyan), south China during the last 68 ka: implications for environmental and climatic change. *Organic Geochemistry* 34, 1497-1515 (2003).
22. Schaller, T., Moor, C. H. & Wehrli, B. Sedimentary profiles of Fe, Mn, V, Cr, As and Mo as indicators of benthic redox conditions in Baldeggersee. *Aquatic Science* 59, 345-361 (1997).
23. Davison, W. Iron and manganese in lakes. *Earth Sci. Rev.* 34, 119-163 (1993).
24. Dykoski, C. A. et al. A high-resolution, absolute-dated Holocene and deglacial Asian monsoon record from Dongge Cave, China. *Earth Planet. Sci. Lett.* 233, 71-86 (2005).
25. Wang, Y. et al. The Holocene Asian Monsoon: Links to solar changes and North Atlantic Climate. *Science* 308, 854-857 (2005).